JOURNAL OF OPTOELECTRONICS AND ADVANCED MATERIALS Vol. 9, No. 12, December 2007, p. 3821 - 3826

Synthesis of calcium phosphate thin layers of increased biological activity by chemical growth in simulated body fluids

J. NEAMTU, G. E. STAN[a], C. MOROSANU[a,*], C. DUCU[b], A. POPESCU[c], I. N. MIHAILESCU[c]
University of Medicine and Pharmacy, Craiova, Romania
[a]*National Institute for Materials Physics, Bucharest-Magurele, Romania*
[b]*University of Pitesti-Research Center for Advanced Materials, Pitesti-Arges, Romania*
[c]*National Institute for Lasers, Plasma and Radiation Physics, Bucharest-Magurele, Romania*

We studied the chemical growth of calcium phosphate nanostructured coatings onto silicon wafers pre-covered with carbonated polycrystalline hydroxyapatite films. Silicon wafers were covered with hydroxyapatite thin layers by radio frequency magnetron sputtering and then immersed in 37º C simulated body fluids for up to 20 days. Immersed structures were extracted every 2 days for studies by Fourier transform IR spectrometry. The chemically grown layers were further analyzed by X-ray diffraction and scanning electron microscopy. The growth kinetics of calcium phosphate deposits was monitored by estimating the area of phosphate, carbonate and water stretching bands of the recorded infra-red vibrational spectra. Sequential annealing in vacuum up to 950 °C was applied to elucidate the nature of incorporated water. Our studies revealed that the layers growing in simulated body fluid are rougher than initial hydroxyapatite interlayers, contain carbonates, include water in interlayer's voids and have therefore an increased biological activity for promoting faster implants integration with human bone tissues.

(Received October 8, 2007; accepted December 4, 2007)

Keywords: Biomimetic metal implants, Calcium phosphate bioactive coatings, Chemical growth in SBF, Rf-magnetron sputtering

1. Introduction

During recent years the synthesis and characterization of thin hydroxyapatite [HA, $Ca_{10}(PO_4)_6(OH)_2$] nanostructured layers focused the interest of an intense fundamental and applied biomedical research.

The eligibility premises of HA nanostructures are based upon their close resemblance to the chemical bone constituents which are in fact carbonated HA including different elemental traces.

Radio-frequency magnetron sputtering deposition (rf-MS) [1, 2] represents a viable alternative to plasma spraying [3, 4] (already commercial) due to the possibility of obtaining thin HA structures with high adherence, density, uniformity and bioactivity [5, 6, 7, 8].

Also, a good response to *in vivo* tests was anticipated of CaP polycrystalline coatings synthesized by chemical growth in simulated body fluids (SBF) [9, 10].

We therefore performed and report herewith a comprehensive kinetical study of the chemical growth of CaP coatings in SBF onto HA crystallized layers pre-deposited by rf-MS on surfaces of Si wafers.

2. Experimental

2.1 Deposition and annealing

rf-MS films were deposited onto single side polished (100) silicon wafers using a rf (1.78 MHz) magnetron cathode with a plasma ring of about 55 mm diameter. A rather high deposition rate of 0.6 μm/h was applied, suitable for preparing thin coatings for osteointegrating implants.

The targets (110 mm diameter, 1 mm thick), were manufactured from high purity HA powder by semi-dry pressing followed by annealing in air at 300 °C.

The sputtering chamber was in a first step evacuated down to a residual pressure of $\leq 10^{-3}$ Pa. Next, high purity argon (99.99%) was introduced through a needle valve and the gas flow was kept at a value of 45 sccm. The corresponding dynamic pressure monitored, with a capacitive Alcatel AS 1004 gauge, was 0.2 Pa.

Calcium phosphate coatings of around 300 nm were deposited during 30 min choosing a target to substrate distance of 35 mm. The deposited films were further annealed in environmental air at 550° C for 60 min in order to enhance their crystallization process. The obtained HA structures were used as seed layers for promoting the chemical growth in SBF at 37° C.

Some of the the grown up samples in SBF were annealed in environmental air for 15 minutes at 200, 300, 500, 600, 800 or 950 °C in order to elucidate the nature of incorporated water molecules. The introduction /extraction in and from annealing furnace have been carried on slowly enough, in order to avoid the film's damage.

2.2. Studies in SBF

SBF solutions have been prepared by subsequently dissolving in deionised water the reagent grade chemicals in the order: NaCl, $NaHCO_3$, KCl, $Na_2HPO_4.2H_2O$, $MgCl_2.6H_2O$, $CaCl_2.2H_2O$ and Na_2SO_4. The synthesis

fluid was buffered at pH=7.4 and 37° C with tri-hydroxymethyl-aminomethane $(HOCH_2)_3CNH_2$) and 1M hydrochloric acid (HCl) solution [11, 12]. Indicative comparative data of ion concentrations in SBF vs human blood plasma are given in Table 1.

Table 1. Ionic concentrations of SBF and human blood plasma.

Concentration (mM)	Ions	Human Sanguine Plasma	SBF
	Na^+	142.0	142.0
	K^+	5.0	5.0
	Ca^{2+}	2.5	2.5
	Mg^{2+}	1.5	1.5
	HPO_4^{2-}	1.0	1.0
	Cl^-	103.0	125.0
	HCO_3^{2-}	27.0	27.0
	SO_4^{2-}	0.5	0.5

Before immersion in SBF, all samples were rinsed with deionised water, cleaned in an ultrasonic bath with acetone and ethanol, rinsed again with deionised water and then dried at 40 °C. The samples were then immersed in 1000 ml SBF, at 37° C, in a thermostatically controlled environment. They were successively extracted every two days from SBF. This procedure was used instead of classical 1, 3, 7, 14, 21 days extraction in order to better reveal some important features of the chemical growth process, as e.g., the dissolution of the HA film in the first 2-3 days, the linear increase/saturation of the chemical grown calcium phosphate deposits, or the appropriate monitoring of the chemical growth process kinetics to avoid the differences between the sputtered seed samples which might appear in classical Kokubo procedure.

2.3 Investigations of obtained structures

All samples were characterized in transmission by Fourier transform infrared spectrometry (FTIR) using a Nicolet AVATAR 320 apparatus. Before and after the chemical growth the samples have been investigated by X-ray diffraction (XRD) using a DRON UM1 diffractometer connected to a PC. A horizontal powder goniometer with graphite monochromator was used in Bragg-Brentano focusing geometry. The incident Cu-K_α radiation, λ = 1.54178 Å, was applied at 35 kV and 30 mA. The typical acquisition conditions were: 5s / step, investigation angle 2θ within the range (20-150°), with a resolution step of 0.05°.

After annealing in ambient air and chemical growth in SBF, the obtained structures were analyzed by Scanning Electron Microscopy (SEM) with Energy Dispersive Spectrometry (EDS). These provide information about the topography and the composition of bioactive structures

3. Results and discussion

3.1 SEM and EDS data

According to SEM observations, deposited crystalline HA films were rather smooth (Fig. 1a) as characteristic to structures obtained by rf-MS. Nevertheless, one can notice a strong nanostructuring of surface with grains of (100 – 200) nm in size. Due to poor adhesion to substrate, the peeling of some films was noticed during crystallization. An average Ca/P molar ratio of 1.38 was estimated from EDS measurements of sputtered films.

After 20 days of chemical growth in SBF, the films morphology has changed dramatically (Fig. 1b). Instead of small crystalline grains, the surface is covered by nanoparticle agglomerates without regular shape. Besides, one can notice the presence of high dimension conglomerates up to 1 μm. The topography suggests a chemical grown material with voids and poor mechanical properties.

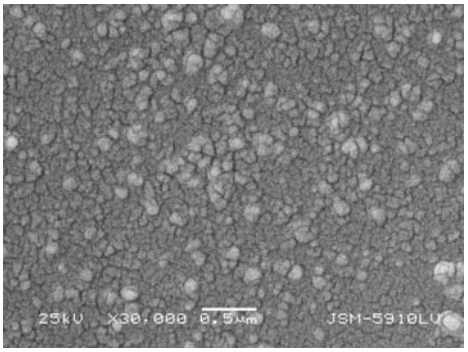

a

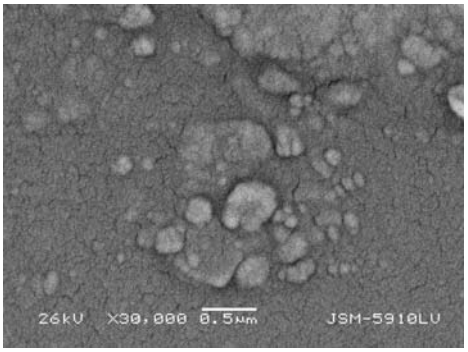

b

Fig. 1. Typical SEM micrographs of as-sputtered HA layer (a) and chemically grown structure after 20 days immersion in SBF (b).

3.2 XRD investigations

We give in Figs. 2 and 3 typical diffraction patterns recorded in case of as-deposited films and respectively of structures after 20 days chemical growth in SBF. We notice in case of as-deposited films by rf-MS the peaks characteristic to HA pointing to a texturing parallel to (002) crystalline plane. Another important observation is

that the crystalline structure remains rather similar after chemical growth in SBF. Nevertheless, a more accurate comparison between the two Figures put however into evidence higher but broader peaks after chemical growth. This could be assigned to a larger amount of synthesized HA but in a poorer crystalline status, probably combined with the absence of texturing.

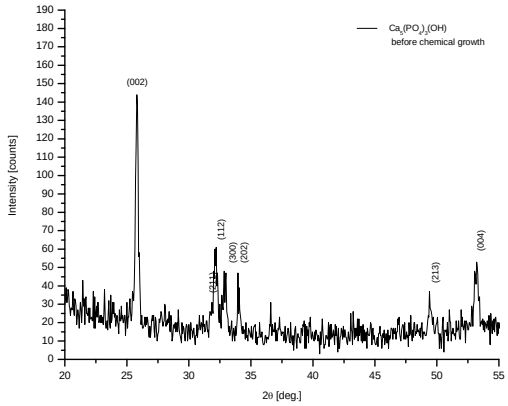

Fig. 2. Typical XRD pattern of as- deposited r f-MS sample.

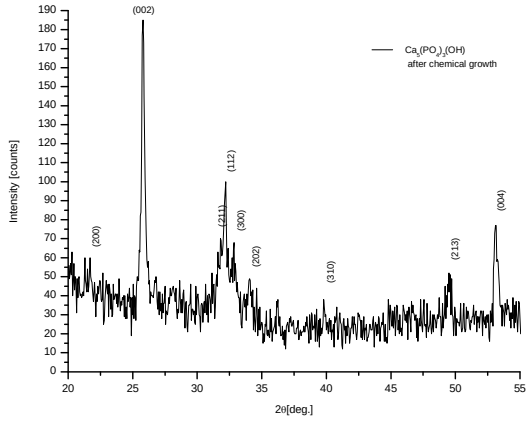

Fig. 3. Typical XRD pattern of rf-MS HA deposited sample after 20 days chemical growth in SBF.

3.3 FTIR spectrometry studies

We give in Fig. 4 typical FTIR spectra recorded in case of rf-MS deposited samples before (a) and after 20 days immersion (b) in SBF. All peaks characteristic to vibration modes of either phosphate [13], OH or carbonate groups are visible in Fig. 4.

Before immersion, the spectrum displayed (ν_3) asymmetric vibration lines corresponding to $(PO_4)^{3-}$ group, intense band at 1031 cm^{-1} and moderate band at 1084 cm^{-1}. These phosphate asymmetric stretching bands are clearly separated - a characteristic to well crystallized structures [13, 14]. A similar splitting of lines was also noticed in the case of asymmetric bending modes (ν_4) at 571 and 599 cm^{-1}. The small peak at 958 cm^{-1}, corresponds to the symmetric stretching (ν_1) mode. No sign of either carbonation or incorporated water was evidenced in case of as-sputtered samples.

After 20 days of immersion in SBF, the area of asymmetric stretching region is increased about three times due to the depositions of CaP's chemical grown onto sputtered HA films. The absence in this case of any separation between ν_3 lines is indicative for a chemical grown disordered structure. The same feature results when comparing the ν_4 bending mode region in Fig. 4a and b. The new chemically growing structure is carbonated as demonstrated by the presence of the $(CO_3)^{2-}$ asymmetric stretching lines (ν_3) at 1509, 1467, and 1421 cm^{-1}. The carbonation is also supported by the appearance of asymmetric bending mode (ν_2) at 877 cm^{-1} [13]. This is the most probably the consequence of the presence of $NaHCO_3$ in SBF. The structure is hydroxylated as shown by presence of the water molecules vibration modes (stretching at 3572 cm^{-1} and bending at 1636 cm^{-1}). Moreover, this spectrum also displays a rather intense and broad absorption band around 3500 cm^{-1} indicating a large number of water molecules and/or (OH) radicals incorporated in films.

From Fig. 5 we noticed a continuous modification of recorded FTIR patterns during samples immersion in SBF.

Quantitative information inferred by a comparative analysis of the patterns in Fig. 5 are provided in Figs. 6-8, where the variation vs. time of the areas of stretching bands of the peaks corresponding to the PO_4, CO_3 and H_2O radicals are given.

The decrease in the first two days (Fig. 6) of the phosphate area points to a slight dissolution of some atomic layers on samples surface prior to the chemical growing process in SBF [15, 16]. This phenomenon stays at the origin of SBF saturation at the solid-liquid interface, promoting the further apatite ingrowths. During the following 2÷10 days the thickness of the chemical amorphous calcium phosphates deposition increases continuously, and saturates after 12 days. At the end of the 20 days period, the area of the phosphate peaks increased almost three times, suggesting the growth of a 900 nm thick layer. This continuous increase of intensity of phosphate bands in SBF (Fig. 6) provides a strong argument in favour of bioactive behavior of growing layer surface.

From FTIR spectra we clearly identified a carbonation band centred at 1400-1500 cm^{-1}. It belongs to the stretching vibration mode of the carboxyl group. We displayed in Fig. 7 the variation of the area of this band during chemical growth in SBF. We notice again a continuous increase exhibiting a saturation tendency after 10 days and reaching its maximum at the end of the period (20 days).

The ratio between the phosphate and carbonate peaks area was calculated from Figs 6 -7 in order to evaluate the uniformity of the carbonation during the chemical growth process. This ratio which is initially infinite for as deposited HA layers rapidly stabilizes to a value of about

450. This suggests that during chemical growth a constant balance between phosphate vs. carbonate is reached.

The increase of the hydroxyl peaks visible in Fig. 8 proves that water molecules were continuously incorporated from SBF into the apatite film growing onto HA deposited layer. The saturation of the H_2O peak area takes place between 10^{th} to 12^{th} days, similar to $(PO_4)^{3-}$ peaks (Fig. 6).

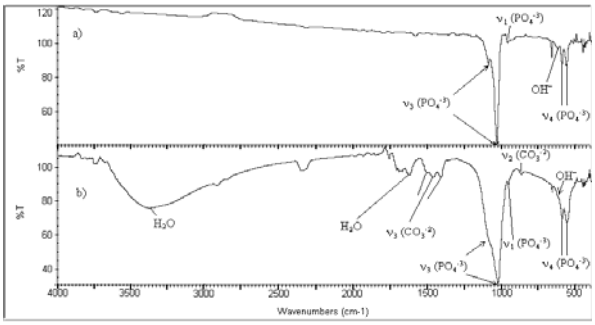

Fig. 4. FTIR spectra of the rf-MS deposited samples before (a) and after (b) the three weeks immersion in SBF.

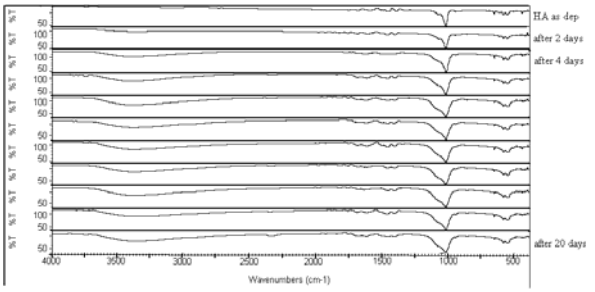

Fig. 5. FTIR spectra of the immersed samples, recorded each 2 days till day 20.

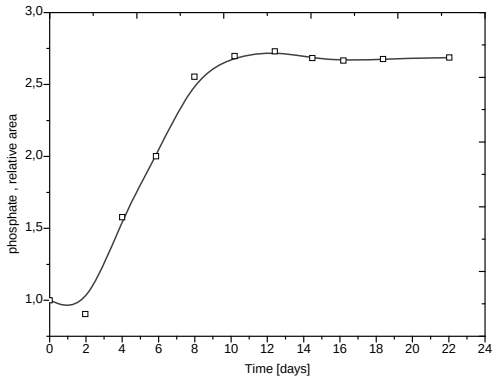

Fig. 6. Time evolution of the phosphate stretching bands area recorded every two days during chemical growth in SBF.

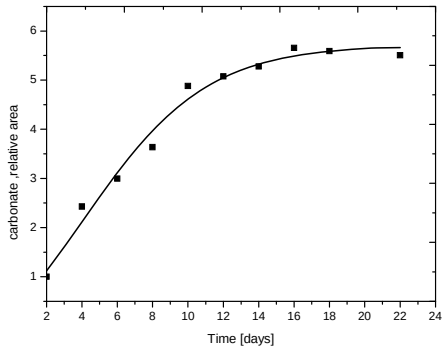

Fig. 7. Time evolution of the carbonate stretching bands area recorded every two days during chemical growth in SBF.

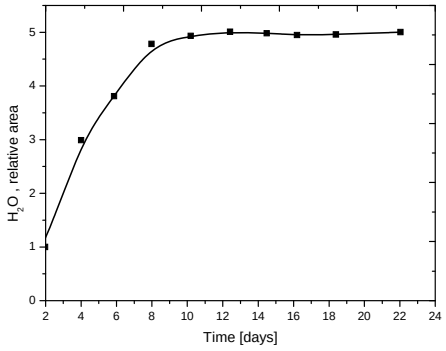

Fig. 8. Time evolution of the water stretching bands area recorded every two days during chemical growth in SBF.

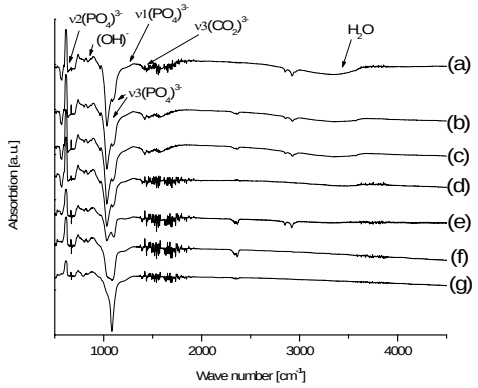

Fig. 9. FTIR spectra recorded for the SBF grown samples 20 days annealed for 15 minutes at (b)-200, (c)-300, (d)-500, (e)-600, (f)-800, and (g)-950^o C.

In order to elucidate the nature of water incorporated into chemically grown layer successive annealing were performed at temperatures up to 950 °C. Fig. 9 displays the FTIR transmission spectra recorded after annealing for 15 minutes at 200, 300, 500, 600, 800, and 950 °C. We observe an obvious decrease of both water and carboxyl stretching lines intensity with increasing temperature.

More precisely the area of carboxyl and water vibration bands strongly decreases up to 500 °C, while the shape of $(PO_4)^{3-}$ lines slightly changed. Indeed, above 500 °C up to 800 and 950 °C, the $(PO_4)^{3-}$ stretching lines became more and more narrow.

To get more quantitative information, we further evaluated both the area of water stretching lines between (3700 – 2900) cm^{-1} and of the phosphate vibration lines at 1031 – 1084 cm^{-1}. We deconvoluted the stretching band of $(PO_4)^{3-}$ radical line for samples annealed at 600, 800 and 950 °C. Our aim was to evidence the expected increase following annealing of the short range order in the crystalline hydroxyapatite structure. We selected these samples because the ones annealed at lower temperatures have a bilayer structure with different degrees of crystallinity. For chosen samples we succeeded a suitable deconvolution with symmetrical and asymmetrical $(PO_4)^{3-}$ radical vibration bands and the asymmetrical SiO_2 radical vibration band. An example is given in Fig. 10 for the chemical grown sample heat treated at 800 °C. The short range order in hydroxyapatite structure was further monitored by the values of τFWHM for the 1080 cm^{-1} line visible in Fig. 10, but also present in case of samples annealed at 600 and 950 °C.

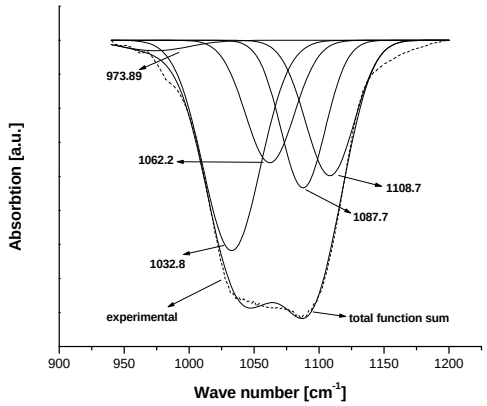

Fig. 10. Deconvolution of $(PO_4)^{3-}$ stretching band of the sample annealed at 800 °C with Gaussian shape lines.

The dependence on temperature of the τ FWHM duration is presented in Fig. 11. We also displayed in Fig. 11 the time variation of the ratio between the areas of H_2O vs. $(PO_4)^{3-}$ vibrations in case of samples annealed at 200, 300, 500, 600, 800 or 950 °C. We preferred this ratio to the absolute area of the H_2O line in order to avoid the measurement errors due to possible local peeling off phenomena. From Fig. 11, we notice a strong decrease of the two areas ratio up 200 °C, which is the most probably due to the intervoids water elimination. The water traces are completely removed between 200 and 600°, and at 950 °C no line of water was evidenced. We note however that some water incorporation during chemical grown in SBF could be important for the osteosynthesis processes and so, no heating (in any case not in excess of 600 °C) is recommended of structures obtained by rf-MS deposition followed by chemical growth in SBF.

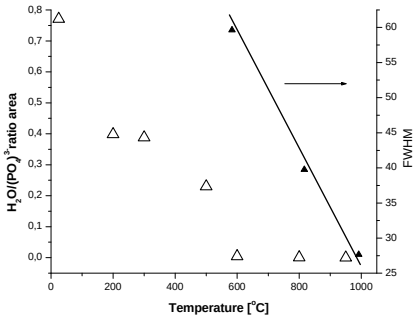

Fig. 11. Dependence on annealing temperature of the ratio between areas of H_2O vs $(PO_4)^{3-}$ bands (left Y axes) and τ FWHM duration of 1080 cm^{-1} line of $(PO_4)^{3-}$ peak in Fig. 10 (right Y axes).

4. Conclusions

Our studies evidenced a strong activity (activation) as an effect of immersion in SBF of crystalline HA thin layers obtained by rf-MS. The layers chemically grown in SBF include carbonates to the difference of the initial HA thin films deposited by rf-MS. The inclusion of carbonates is rather uniform during the whole immersion process in SBF (of 20 days). The resulting over layer is therefore closer and more compatible to the actual (human) bone structure containing carbonates. The growing apatite also incorporates unbound water inside layer's voids, as demonstrated by the successive annealing steps up to 950 °C.

The main inferring of our study is that the chemical growth in SBF favors the synthesis and deposition of an overlayer with structure and composition more similar to the actual (human) bone and therefore of an expected increased biological activity and more suitable for the active proliferation and differentiation of osteoblast cells.

Acknowledgements

We acknowledge the support of the Romanian Ministry of Research and Technology as well as the R &D framework programs: CERES (project 3-124) and VIASAN (project CEEX 151).

References

[1] T. Yamaguchi, Y. Tanaka, A. Ide-Ektessabi, Nucl. Instr. and Meth. B **249**, 723–725 (2006).
[2] V. Nelea, C. Morosanu, M. Iliescu, I. N. Mihailescu, Surf. Coat. Technol. **173**, 315-322 (2003).
[3] Y.-P. Leea, C. K. Wangb, T.-H. Huanga, C. C. Chena, C. T. Kaoa, S.-J. Ding, Surf. Coat. Technol **197**, 367–374 (2005).
[4] J. Wenga, M. Wanga, J. Chen, Biomaterials **23**, 2623–2629 (2002).

[5] S.-J. Ding, Biomaterials **24**, 4233–4238 (2003).
[6] E. S. T. Himeno, T. Kokubo, T. Nakamura, Biomaterials **26**, 4366–4373 (2005).
[7] S.-J. Ding, C.-P. Ju, C. Lin, J. Mater. Res. **47**, 551-563 (1999).
[8] L. Verestiuc, C. Morosanu, I. Pasuk, M. Bercu, I. N. Mihailescu, J. Crystal Growth 264/1-3, 483-491 (2004).
[9] H.-M. Kima, H. Takadama, Biomaterials **27**, 2907–2915 (2006).
[10] T. KokuboThiana, J. Huanga, S. M. Besta, Z. H. Barberb, W. Bonfield, Biomaterials **26**, 2947–2956 (2005).
[11] T. Kokubo, H. Kushitani, S. Sakka, T. Kitsugi, T. Yamamuro, J. Biomed. Mat. Res. **24**, 721–734 (1990).
[12] L. Hench, J. Wilson, in "An introduction to bioceramics", (World Scientific Publishing Co., Pte. Ltd., 1999).
[13] M. Markovic, B. O. Fowler, M. S. Tung, J. Res. Natl. Inst. Stand. Technol. **109**, 553-568 (2004).
[14] C. W. Yang , T.-S. Lui, E. Chang, Advanced Materials Research 15-17, 147-152 (2007).
[15] Y. R. Duan, Z. R. Zhang, C. Y. Wang, J. Y. Chen, X. D. Zhang, J. Mat. Sci: Mater. Med. 15, 1205-1211 (2004).
[16] M. Vaahtio, T. Peltola, T. Hentunen,; H. Ylänen, S. Areva, J. Wolke, J. Mat. Sci: Mater. Med. **17**, 1113-1125 (2006).

*Corresponding author: morosanu@infim.ro